RSC Advances

RSC Advances

www.rsc.org/advances

ROYAL SOCIETY OF CHEMISTRY

www.rsc.org/advances

Journal Name

ARTICLE

Nanonet-structured poly(*m*-phenylene isophthalamide)-polyurethane membranes with enhanced thermostability and wettability for high power lithium ion batteries

Ke Xiao,[‡a] Yunyun Zhai,[‡ab] Jianyong Yu[c] and Bin Ding [*ac]

To solve the thermal shrinkage, flammability and wettability problems of conventional polyolefin separators, we have prepared the nanonet-structured poly(m-phenylene isophthalamide)-polyurethane (PMIA-PU) nanofibrous membranes with enhanced thermostability and good wettability for high power lithium ion batteries (LIBs) via one-step electrospinning technique. The as-prepared PMIA-PU membranes demonstrate improved mechanical strength (>15.79 MPa) and high ionic conductivity up to 1.38 mS cm^{-1} due to the introduction of PU and the formation of nanonet-structure. Benefiting from the introduction of PMIA, the as-prepared PMIA-PU membranes were endowed with not only improved thermostability and nonflammability but also excellent wettability to liquid electrolyte, which could be beneficial for improving the safety and reliability of LIBs. Moreover, the excellent affinity between the carboxy group (PMIA and PU) and the carbonate ester group of liquid electrolyte enables the PMIA-PU membranes with good anodic stability up to 4.86 V. More importantly, the PMIA-PU membrane based Li/LiFePO$_4$ cell exhibits comparable cycling stability delivering a discharge capacity of 160 mA h g^{-1} at the 65th cycle and better rate capability compared with the Celgard membrane based cell. These results indicate a very promising direction for the safe and reliable separators, which may make further progress in obtaining the enhanced performance of LIBs.

Introduction

The development of new materials has hastened the improvements in lithium ion batteries (LIBs) over the past decades, providing exciting opportunities for high-power and high-energy density devices.[1,2] As critical components of rechargeable LIBs, separators not only play an important role in preventing the physical contact between electrodes to avoid short circuit even at elevated temperature but also providing a path for free ionic transport via liquid electrolyte-filled pores.[3-5] Therefore, the properties of the separator not only determining the electrochemical properties but also influencing the safety of LIBs.

Currently, the polyolefin membranes have been the most predominant one in commercial LIBs owing to their low cost, high mechanical strength, good electrochemical stability and thermal shutdown performance.[5] Nevertheless, their intrinsically low thermostability at elevated temperature due to the relatively

low softening and melting temperature,[3] which triggers internal shorting between electrodes, results in the thermal runaway and eventually incurs safety issues.[6] Moreover, their intrinsic hydrophobicity and low surface energy result in poor wettability to polar liquid electrolyte, and thus restricting their applications in high power LIBs.[3,5] Therefore, it is highly desirable to fabricate membranes with enhanced thermostability and good wettability to guarantee the safety and reliability of LIBs.[7]

To solve the above-mentioned drawbacks of polyolefin membranes, various methods have been developed to fabricate alternatives of polyolefin membranes, including phase separation,[8-10] hard template,[11] and paper-making.[12,13] Notice that these methods are difficult-to-control, time-consuming and energy-intensive. Electrospinning, as an alternative to these methods, has been considered a promising technology to prepare membranes with excellent thermostability and good electrolyte wettability. Electrospun membranes possess interconnected pore

structure with high porosity, and thus absorbing large amounts of liquid electrolytes and offering effective conduction channels, which in turn are endowed with high ionic conductivity and good electrochemical properties.[5,14,15] Taking into consideration of these intriguing characters, novel electrospun nanofibrous membranes including polymethylpentene[16], polyimide,[17,18] and cellulose[19] have been studied. However, the practical application of these membranes is limited by the low tensile strength and the loss of thermal shutdown function. Therefore, continuing efforts of seeking ideal separator for high-power LIBs needs to be further devoted.

Poly(*m*-phenylene isophthalamide) (PMIA) is a polymer with meta-type benzene-amide linkages in its skeletal chain (Fig. S1), thus leading to extremely high thermostability up to 400 °C,[20] which can effectively avoid short circuits caused by the shrinkage of the separators. Moreover, the carboxy group of PMIA exhibits strong affinity toward the carbonate ester solvent molecules of liquid electrolyte due to the similar polarity. Polyurethane (PU), a class of thermoplastic polymer that contains two-phase microstructure (soft segments and hard segments) (Fig. S2), is chosen as the polymer for the preparation of separators with high ionic conductivity.[21] Therefore, it is a potential strategy to prepare PMIA-PU based membranes as separators for high power LIBs.

In the current work, we have prepared the nanonet-structured PMIA-PU nanofibrous membranes for high power LIBs via electrospinning technique. The PMIA-PU membranes demonstrate high ionic conductivity and improved mechanical strength due to the formation of nanonet-structure and the introduction of PU. Benefiting from the introduction of PMIA, the as-prepared PMIA-PU membranes were endowed with not only improved thermostability and nonflammability but also excellent wettability to liquid electrolyte. Our work may provide a new direction for the development of electrospun nanofibrous membranes used in high power LIBs.

Experimental

Materials

PMIA (Teijinconex®) was supplied by Teijin Ltd., Japan. Polyurethane (PU, Elastollan 2280A10) was purchased from BASF Co., Ltd. N,N-dimethylacetamide (DMAc) was obtained from Shanghai Lindi Chemical Reagents Co., Ltd., China. Lithium chloride (LiCl) was purchased from Aladdin Industrial Co., China. The Celgard 2320 membrane (Celgard, China) with a thickness of about 20 μm were used as the separator for a comparative study. All chemicals were of analytical grade and used as received without further purification.

Fabrication of PMIA-PU composite membranes

LiCl/DMAc ionic liquid was used as the solvent for PMIA, the concentration of PMIA and LiCl in the precursor solution were 15 and 2 wt%, respectively. The PU solution with a

concentration of 7 wt% was prepared by dissolving PU into DMAc with stirring for 12 h at room temperature. Then, the PMIA and PU solutions were mixed together to make homogeneous solutions in which the weight ratios of PMIA and PU are 2/8, 4/6, 6/4 and 8/2, respectively. The representative setup for the preparation of PMIA-PU composite separators was performed by using the DXES-3 spinning equipment (Shanghai Oriental Flying Nanotechnology Co., Ltd., China). The PMIA-PU blended solution was loaded into a syringe and injected through a plastic needle with a flow rate of 0.2 mL h⁻¹. A high voltage of 30 kV was applied to the needle tip and the distance between the spinneret and an aluminum foil-covered grounded rotating collector (rotating rate of 100 rpm) was fixed at 25 cm. The ambient temperature and relative humidity were 23±2 °C and 45±3%, respectively. Then, the free-standing fibrous membranes were dried at room temperature on the collector for 6 h to prevent the further shrinking and then removed from the collector. The resulting PMIA-PU composite membranes were dried in a vacuum oven at 70 °C for 12 h to remove the residual solvent and transferred to a dry box for further use.

Characterization of PMIA-PU composite membranes

High resolution field-emission scanning electron microscope (FE-SEM, S-4800, Hitachi Ltd., Japan) was used to observe the morphology of relevant membranes. The average pore diameter and pore size distribution of as-prepared membranes were measured by a bubble-point test performed on a capillary flow porometry (CFP-1100AI, Porous Materials Inc., USA). Water contact angle measurements were performed by a contact angle goniometer Kino SL200B equipped with tilting base. The mechanical properties of the membranes were performed on a tensile tester (XQ-1C, Shanghai New Fiber Instrument Co., Ltd., China). Thermal shrinkage was evaluated after storing the relevant membranes in an oven at various temperatures from 90 to 180 °C for 0.5 h, after that, dimensional change of the membranes were carefully measured by the following equation:

$$Shrinkage(\%) = \frac{A_0 - A}{A_0} \times 100 \quad (1)$$

where, A_0 and A are the initial and final areas of relevant membranes, respectively. Porosity (P) of the PMIA-PU membranes was determined by using *n*-butanol uptake tests and then calculated by the following equation:

$$P(\%) = \frac{M_{BuOH}/\rho_{BuOH}}{(M_{BuOH}/\rho_{BuOH}) + (M_m/\rho_m)} \times 100 \quad (2)$$

where M_m and M_{BuOH} are the mass of the dry membranes and *n*-butanol absorbed, ρ_{BuOH} and ρ_p are the densities of *n*-butanol and membranes. The electrolyte uptake was measured by the weight difference of membranes before and after liquid electrolyte (1 M lithium hexafluorophosphate (LiPF₆) dissolved in ethylene carbonate (EC)/dimethyl carbonate (DMC)/ethyl methyl

carbonate (EMC) (1/1/1, w/w/w), provided by Guangzhou Tinci Materials Technology Co., Ltd.) soaking for 2 h and then calculated according to the following equation:

$$Uptake(\%) = \frac{W_w - W_d}{W_d} \times 100 \quad (3)$$

where W_d and W_w are the mass of the PMIA-PU membrane before and after fully swelling in electrolyte, respectively.

Electrochemical performance evaluation

Ionic conductivity (σ) of relevant membranes was tested by electrochemical impedance spectroscopy using the Zahner IM 6ex impedance analyzer. The impedance measurements were performed on liquid electrolyte-soaked membranes sandwiched between two stainless steel (SS) blocking electrodes over the frequency range from 0.1 Hz to 1 MHz at an amplitude of 5 mV. The ionic conductivity could be calculated from the following equation:

$$\sigma = \frac{d}{R_b \times S} \quad (4)$$

where d is the thickness of relevant fibrous membranes, which was measured by an electronic micrometer (0.001 mm accuracy, CHY-C2 Thickness Tester, Labthink Co. Jinan, China), R_b is the bulk resistance obtained at the high frequency intercept of the Nyquist plot on the real axis, and S is the area of the stainless steel blocking electrode. The MacMullin number (N_m) and tortuosity (τ) of membranes can be calculated by the following equation:

$$N_m = \frac{\sigma_0}{\sigma_{eff}} \quad (5)$$

$$\tau^2 = N_m P \quad (6)$$

where, σ_0 and σ_{eff} are the ionic conductivities of liquid electrolyte (8.72 mS cm^{-1}) and liquid electrolyte soaked membranes, P is the porosity of relevant membranes. The anodic stabilities of the liquid electrolyte-soaked membranes were conducted by a linear sweep voltammetry using a stainless steel as working electrode and a lithium piece as counter and reference electrode at a scan rate of 5 mV s^{-1} over the potential range from 2.5 to 6.0 V $vs.$ Li$^+$/Li. The CR2016 coin cells were assembled by sandwiching separators between a LiFePO$_4$ cathode (LiFePO$_4$/carbon black/PVdF, 80/10/10, w/w/w) and a lithium metal anode. The mass loading of LiFePO$_4$ was about 8 mg cm^{-2}, much higher than that for the most reported, about 2 mg cm^{-2}. All the assembly processes of cells were carried out in an argon-filled glovebox with oxygen and moisture level <1 ppm. The battery performance of the Li/LiFePO$_4$ cells using the Celgard membrane and PMIA-PU membranes were conducted in a Land battery test system (CT 2001A, Wuhan Land Electronic Co. Ltd., China) by charging to 4.0 V under a constant current-constant

voltage mode and discharging to 2.5 V in a constant current mode at room temperature.

Results and discussion

Morphology

Fig. 1 presents the typical surface morphology of the as-prepared PMIA-PU based membranes fabricated from different weight ratios of PMIA-PU. As expected, the PMIA-PU nanofibers are randomly deposited as three-dimensional tortuous pore structures in the form of nonwoven, which may play an important role in decreasing the current leakage. By varying the weight ratios of PMIA-PU from 2/8 to 8/2, the average diameters gradually decrease from 292 to 217 nm. Interestingly, the formation of spider-web-like nano-nets can be observed among the fibers, and the coverage rates of nano-net decrease with increasing PMIA contents. Moreover, as seen from Fig. 1a-d, the adhesions among the adjacent fibers gradually decrease with increasing PMIA contents. The introduction of PU and the incomplete evaporation of DMAc result in the formation of bonding structure, which is beneficial for enhancing the tensile strength of PMIA-PU membranes.

Pore size and pore size distribution

The pores of separators for LIBs should be small enough to prevent dendritic lithium penetration through them, and membranes with submicrometer pore sizes have proven satisfactory for LIBs.[3] Fig. 2 shows the mean pore sizes and pore size distributions of as-prepared PMIA-PU membranes with varied weight ratios. All the PMIA-PU membranes have displayed narrow pore size distribution concentrating in the range of 0.1-1.1 μm, and the mean pore size gradually increases from 0.43 to 0.91 μm with the increasing PMIA content (Table 1), which are lower than the mean pore sizes of electrospun PVdF nanofibers.[22,23] The differences in mean pore sizes and
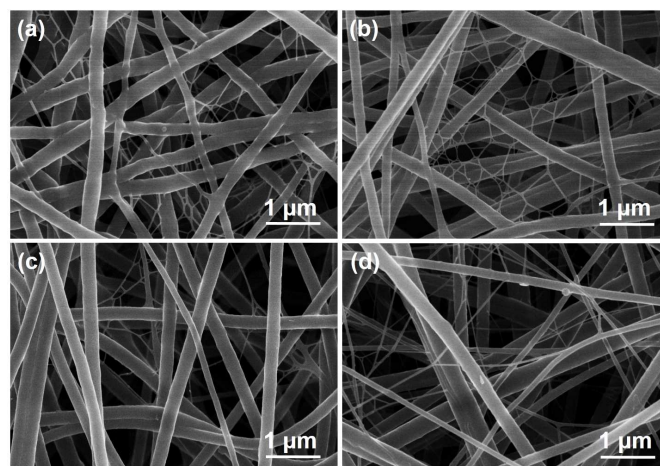
Fig. 1 FE-SEM images of as-prepared PMIA-PU membranes fabricated from varied weight ratios of (a) 2/8, (b) 4/6, (c) 6/4 and (d) 8/2

Table 1 Brief physical properties of PMIA-PU based nanofibrous separators.

Weight ratio of PMIA/PU	Mean pore size (μm)	Porosity (%)	Uptake (%)	Ionic conductivity (mS cm^{-1})	MacMullin number	Tortuosity	Ea (kJ mol^{-1})
2/8	0.43	80.34	526.55	0.51	17.10	3.71	1.73
4/6	0.73	88.62	740.03	0.83	10.51	3.05	2.12
6/4	0.77	90.08	843.52	1.38	6.32	2.39	1.48
8/2	0.91	90.43	827.70	0.97	8.99	2.85	1.33
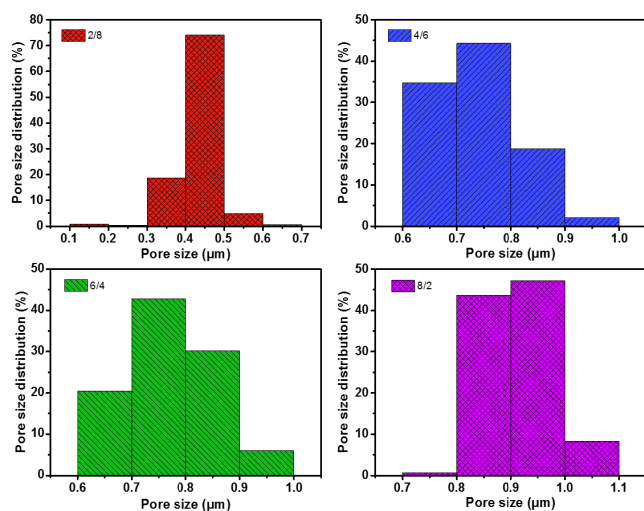
Fig. 2 Pore size distributions of as-prepared PMIA-PU membranes fabricated from varied weight ratios.

Fig. 3 (a) Stress-strain curves of as-prepared PMIA-PU membranes fabricated from varied weight ratios. (b) Twisting and (c) folding tests of resultant PMIA-PU membranes with the weight ratio of 6/4.

pore size distributions may be ascribed to the differences in fiber diameters, the adhesions among adjacent fibers and packing densities.

Mechanical property

The stress-strain curves of as-prepared PMIA-PU nanofibrous membranes are depicted in Fig. 3a. The fracture stress of the PMIA-PU membranes decrease from 25.23 to 15.79 MPa with the increase of PMIA content, which may be due to the less formation of bonding structure (Fig. 1). The result implies that the formation of bonding structure is beneficial for enhancing the fracture stress of PMIA-PU membranes. As can be seen in Fig. 3a, PMIA-PU membranes with weight ratio of 2/8 show different stress-strain curves from the other three PMIA-PU based membranes, but show similar behaviour to PU membranes (Fig. S3). Thus, we can deduce that the different curve of PMIA-PU membranes with the weight ratio of 2/8 was due to the high content of PU. Meanwhile, the introduction of rigid PMIA makes the membranes slightly less flexible and thus leading to the

decreases in elongation at break. The fracture stress of PMIA-PU membranes are lower than the fracture stress in the machine direction (114.28 MPa) but higher than the fracture stress in the transverse direction (12.88 MPa) of Celgard membrane, which are also higher than the most electrospun separators reported in the previous studies.[16,24,25] Moreover, the PMIA-PU membranes could be severely twisted several times without breaking along a glass rod with a diameter of 5 mm (Fig. 3b), and not mechanically ruptured after being fully folded at a bending angle of almost 180° (Fig. 3c), reflecting the superior flexibility of the PMIA-PU membranes. The above results imply that the PMIA-PU membranes possess excellent mechanical strength, which is good enough for practical application in high-performance LIBs.

Dimensional thermal stability and nonflammability

Dimensional change at elevated temperature is one of the most important parameters for separators, which must be considered when choosing separators for designing LIBs, especially for high power/energy ones.[26] Fig. 4 demonstrates the dimensional change of the PMIA-PU membranes at elevated temperature. As can be seen in Fig. 4a, it is noted that the Celgard membrane and the PMIA-PU membranes with weight ratio of 2/8 thermally shrinks severely as the temperature increases from 130 to 180 °C. Even at room temperature, the PMIA-PU membranes with
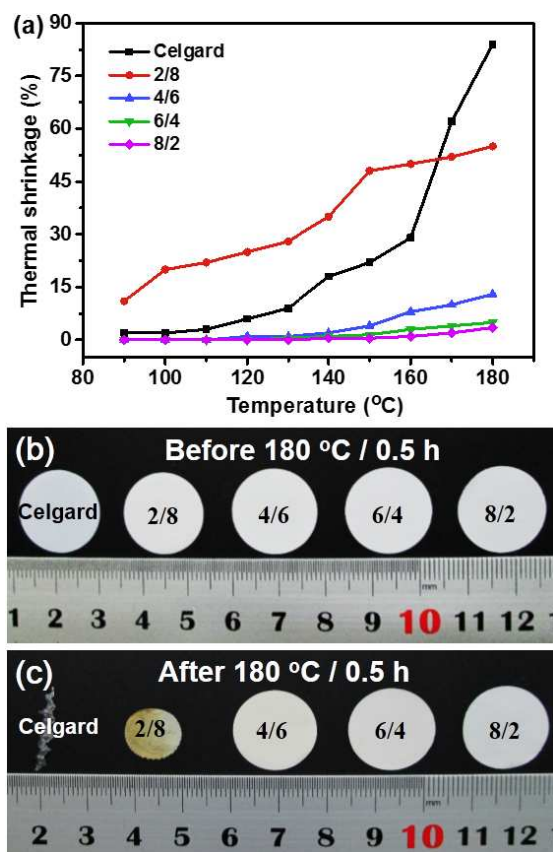
Fig. 4 (a) Comparison of thermal shrinkages of Celgard membrane and as-prepared PMIA-PU membranes as a function of heat-treatment temperature. Photographs of Celgard membrane and as-prepared PMIA-PU based membranes (b) before and (c) after exposure to 180 °C for 0.5 h.

weight ratio of 2/8 shrink nearly 5% (Fig. 4b), which may be attributed to the shrink preference of intrinsic elastic PU after stretching during the electrospinning process. After being stored at 180 °C for 0.5 h, the Celgard membrane shrinks irregularly 84% with the color change from white to transparent due to the shape memory effect caused by the stretching step during the membrane preparation process (Fig. 4b and c). While the dimensional changes of PMIA-PU membranes decrease with the increasing PMIA content, the PMIA-PU membranes with weight ratios of 8/2 and 6/4 show dimensional change of 3.5% and 5% after being stored at 180 °C for 0.5 h, respectively. And the PMIA-PU membranes show isotropic shrinkage because they are composed of random orientation nanofibers. Based on these, we can conclude that the PMIA-PU membranes exhibit better dimensional thermal stability than Celgard membrane, which can be explained by the incorporation of high thermotolerant PMIA. Notably, these results demonstrate that the PMIA-PU membranes would provide the excellent safety characteristics for high power LIBs even at elevated temperature of 180 °C.
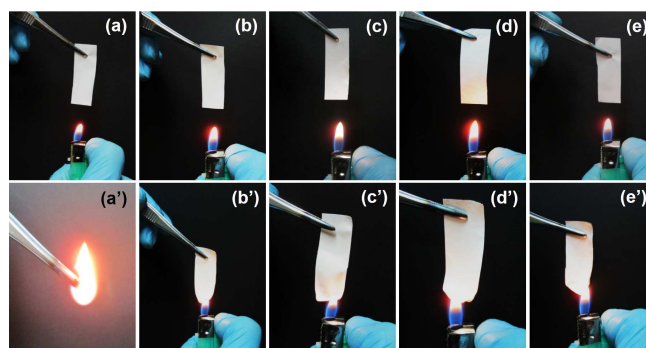
Fig. 5 Combustion tests of (a and a') Celgard membrane and PMIA-PU membranes fabricated from varied weight ratios of (b and b') 2/8, (c and c') 4/6, (d and d') 6/4 and (e and e') 8/2.

The nonflammable property of separators is so crucial that it could terminate further fire or other accident in abuse condition, but it has been rarely mentioned because most separators are combustible, except polyimide based membrane,[17,27] separator prepared using flame retardant,[12] and polymer composed of fluorine or bromine functional groups, such as cellulose/PVdF-HFP,[28] PVdF-glass fiber mats,[8] PVdF-LiPVAOB membranes,[29,30] and brominated poly(phenylene oxide) based separators.[31] The combustion tests of the Celgard and PMIA-PU membranes are presented in Fig. 5, when Celgard is ignited, it is set on fire immediately and completely engulfed in flame. However, the PMIA-PU membranes exhibit perfect flame retarding ability without catching fire, which may be ascribed to the flame retarding and thermal stable characteristics of PMIA. The results indicate that the PMIA-PU nanofibrous membranes are beneficial to enhance the safety characteristics of LIBs.

Porosity, wettability and electrolyte uptake

The porosities of as-prepared membranes vary in the range of 80.34-90.43%, which are much higher than the value of Celgard (49.83%) and silica nanoparticle enhanced polysulfonamide membranes (70%).[32] The wettabilities of the PMIA-PU basedmembranes are evaluated by water contact angle measurements (Fig. 6a). The water contact angles of the PMIA-PU based membranes fabricated from varied weights ratios decreased from 101.06° to 48.91°, implying the increased hydrophilicity with increasing PMIA content. The wetting ability of liquid electrolyte is further confirmed by dropping 1 μL liquid electrolyte on the surface of the separators. As shown in Fig. 6b, the liquid electrolyte forms a bead on the Celgard membrane, whereas, it quickly spread out on the PMIA-PU based membranes, indicating the better affinity of the PMIA-PU membrane to the liquid electrolyte. The excellent wettability could be ascribed to capillary force of the pores in the PMIA-PU nanofibrous membranes and the introduction of hydrophilic
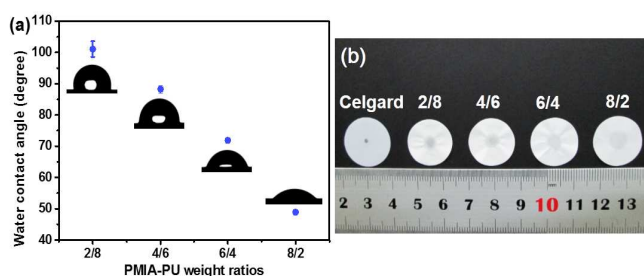
Fig. 6 (a) Water contact angles of PMIA-PU membranes with varied weight ratios. The insets show the corresponding optical profiles of water droplet. (b) Photograph of the wetting behavior of the separators with liquid electrolyte.

PMIA.[33,34] Moreover, the electrolyte uptakes of the PMIA-PU nanofibrous membranes are in the range of 526.55-843.52% (Table 1), which are much higher than that of Celgard membrane. The improved electrolyte uptake is resulted from the high porosity and the strong affinity of the carboxy group (PMIA and PU) toward the carbonate ester group of solvent molecules.[7,35,36]

Ionic conductivity, Mulluin number and tortuosity

One of the most important requirements of separators for LIBs is their ability to transport lithium ion Fig. 7 shows the AC impedance spectroscopies of the liquid electrolyte-soaked Celgard membrane and PMIA-PU nanofibrous membranes determined at 25 °C. As shown in Table 1, the ionic conductivities of PMIA-PU nanofibrous membranes calculated from the impedance spectroscopies shown in the insets of Fig. 7 are in the range of 0.51-1.38 mS cm^{-1}, which are higher than that of Celgard membrane (0.45 mS cm^{-1}), especially for the PMIA-PU nanofibrous membranes fabricated from weight ratio of 6/4. The improved ionic conductivity may be ascribed to the high electrolyte uptake brought by the high porosity and the dissociation of PU to liquid electrolyte.[21] Meanwhile, Fig. 8 depicts the temperature dependence of ionic conductivity of as-prepared PMIA-PU membranes at the temperature range from 30 to 70 °C. It can be observed that the ionic conductivities increase
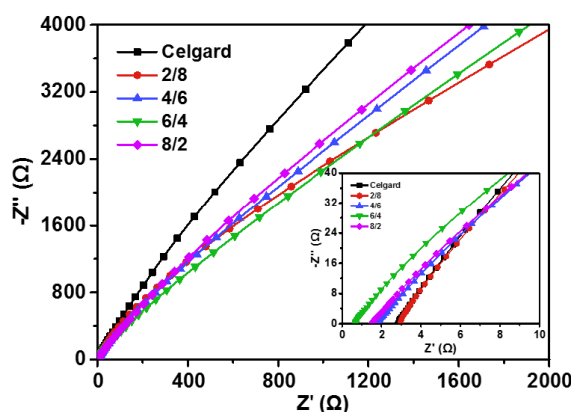
Fig. 7 AC impedance spectra of liquid electrolyte-soaked Celgard membrane and PMIA-PU nanofibrous membranes fabricated from varied weight ratios at 25 °C. Inset shows the plots of high-frequency.
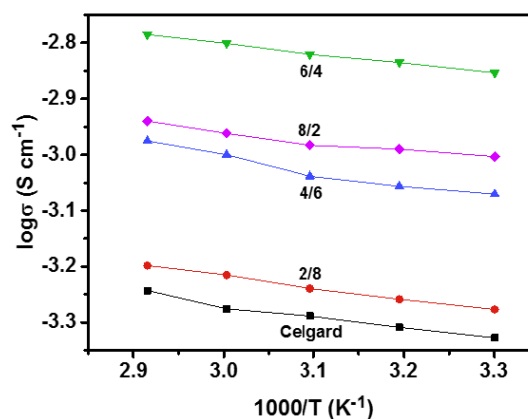
Fig.8 Temperature dependence of ionic conductivities of Celgatd and as-prepared PMIA-PU membranes with varied weight ratios at the temperature range from 30 to 70 °C.

as the temperature increasing, which may be due to the enhanced segmental motion of polymer. The logσ~T curves exhibit a linear relationship, suggesting that conductive behavior of PMIA-PU membranes obeys to Arrhenius equation:

$$\sigma = \sigma_0 \exp(\frac{-Ea}{RT}) \ (7)$$

where R is the gas constant, Ea is the activation energy for effective ionic conduction, σ is the conductivity of polymer electrolyte, σ_0 is the pre-exponential index and T is the testing absolute temperature. As listed in Table 1, the slight differences in calculated Ea values suggest that a little difference in lithium ion conduction of the as-prepared PMIA-PU membranes. The Mulluin number is known to describe a conductivity decrease related to the pore structure and to the affinity between polymer (PMIA and PU) and solvent molecular. The as-prepared PMIA-PU membranes possess the Mulluin numbers in the range of 2.39-3.71, which are much lower than the value of Celgard membrane (19.38),[7,36] implying that the less negative affect of the as-prepared PMIA-PU membranes on the battery performance. Furthermore, the tortuosity values of resultant PMIA-PU membranes are in the range of 2.39-3.71, revealing the high ionic conductivity of PMIA-PU membranes from another point of view. The high ionic conductivities, low MacMullin numbers and tortuosities of as-prepared PMIA-PU membranes would be beneficial for exhibiting stable cycling performance and excellent rate capability.

Anodic stability

The anodic stability tests of Celgard and as-prepared PMIA-PU membranes evaluated by LSV are shown in Fig. 9. There are no obvious increases in anodic current below 4.60 V for Celgard membrane, and the resultant PMIA-PU membranes exhibit higher oxidation potentials in the range of 4.70-4.86 V, revealing that the electrochemical stabilities of PMIA-PU membranes are
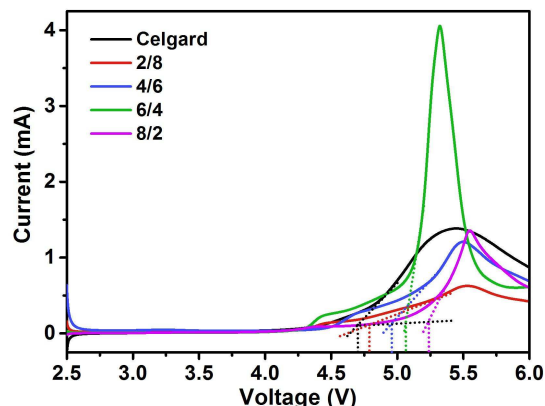
Fig. 9 Anodic stabilities of the cells with Celgard membrane and as-prepared PMIA-PU membranes fabricated from varied weight ratios.

high enough to be used in the high-voltage LIBs. The good electrochemical stabilities of PMIA-PU membranes originate from the excellent affinity between the carboxy group (PMIA and PU) and the carbonate ester group of liquid electrolyte.

Cell performance

The Celgard membrane and as-prepared PMIA-PU membranes with varied weight ratios were applied to Li/LiFePO$_4$ coin cells incorporating high mass loading LiFePO$_4$ electrode of 8 mg cm^{-2}. The assembled cell was initially subjected to a preconditioning cycle over a voltage range of 2.5-4.0 V at a rate of 0.1 C, after 5 cycles, the cells were charged-discharged at 0.2 C rate till 65 cycles. Fig. 10a-c depict the typical charge-discharge curves of the 1st, 30th and 60th cycle of the coin cells using Celgard membrane and PMIA-PU membranes with weight ratio of 2/8 and 6/4, respectively. All the cells demonstrate a pair of well-defined plateaus near 3.38 and 3.5 V, which is charctreristics biphasic Li$^+$ extraction and insertion feature of LiFePO$_4$
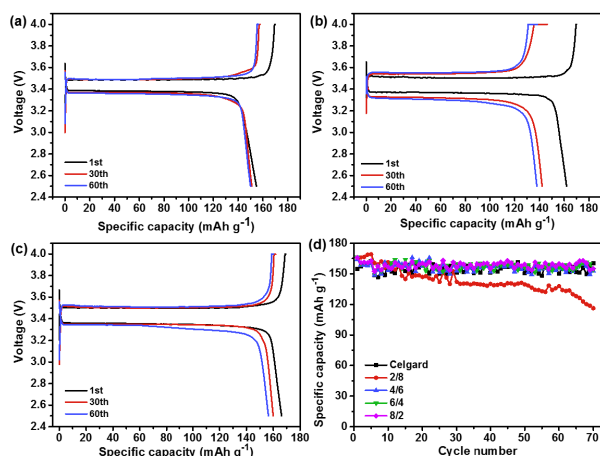
Fig. 10 Charge-discharge curves of Li/LiFePO$_4$ cells assembled with (a) Celgard membrane and PMIA-PU membranes fabricated from weight ratios of (b) 2/8 and (c) 6/4. (d) Cycling stability of Li/LiFePO$_4$ cells assembled with Celgard membrane and PMIA-PU based membranes.
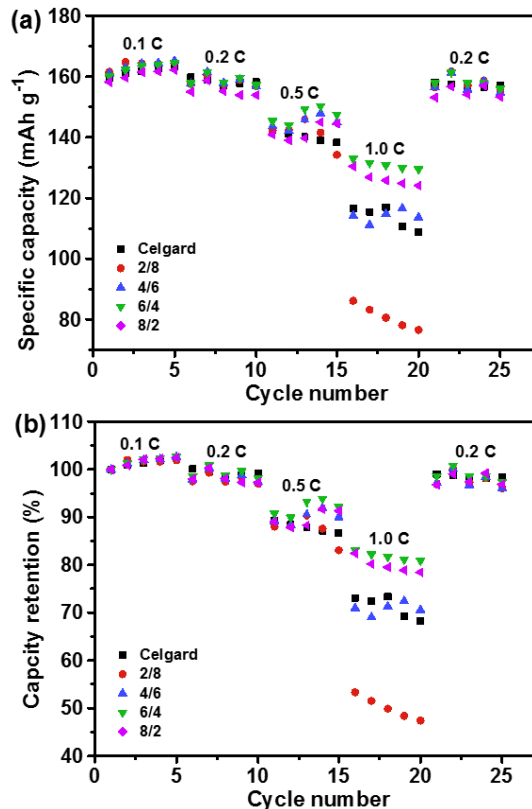
Fig. 11 (a) Discharge rate capabilities and (b) capacity retentions of Li/LiFePO$_4$ cells assembled with Celgard membrane and PMIA-PU membranes fabricated from varied weight ratios.

cathode.[37] The initial discharge capacity of the cell using PMIA-PU membranes with weight ratio of 6/4 is 166.16 mA h g^{-1},which is higher than that of the cells using Celgard membrane (154.78 mA h g^{-1}) and PMIA-PU membranes with weight ratio of 2/8 (161.88 mA h g^{-1}). The differences in discharge capacity is probably due to the differences in the utilization of active materials.[7,38] As shown in Fig. 10d, the cell using PMIA-PU membranes with weight ratio of 6/4 delivers discharge capacity of 160 mA h g^{-1} after 65 cycles, exhibiting the excellent cycling performance. The result is much higher than that of PMIA-PU membranes with weight ratio of 2/8, and comparable to that of Celgard membrane and PMIA-PU membranes with weight ratios of 4/6 and 8/2. The excellent cycling performance of PMIA-PU membranes may be attributed to the high ionic conductivity and electrolyte uptakes caused by their tortuously interconnected porous structure (Fig. 1) and strong affinity of PMIA and PU to liquid electrolyte.

The rate capabilities were also investigated for the cells composed of Celgard membrane and PMIA-PU membranes with varied weight ratios in the range of 0.1 C to 1.0 C as shown in Fig. 11. With an enhanced discharge rate, the discharge capacity capacities decrease regularly, which may be due to the polarization caused by low electronic conductivity of LiFePO$_4$

and limited diffusion of Li^+ in the pores of separators.[7,39] As shown in Fig. 11a, the discharge capacities of all the cells at 0.1 C, 0.2 C and 0.5 C are comparable, and the cells using PMIA-PU membranes with weight ratios of 6/4 and 8/2 deliver higher discharge capacities and capacity retentions (Fig. 11b) with increasing current density (1.0 C), which demonstrates that the ionic conductivity has a significant effect on rate capability.[40] Interestingly, when the rate returns to 0.2 C, the reversible discharge capacities of the above-mentioned cells were both close to the original capacity of 0.2 C rate, indicating that the structural stabilities of the cathode materials are retained.[39] Notably, as shown in Fig. 10b, it seems paradoxical phenomenon that the capacity retention ratios are more than 100% at 0.1 C on occasion, which is attributed to the formation of solid electrolyte interface film. The improved discharge C-rate capability of the cell with PMIA-PU membranes, especially at higher rate, can be explained by their higher ionic conductivities bring by their high porosities, interconnected pore structures and excellent electrolyte wettabilities, which reduce the concentration polarization of the electrolyte and thus delivering higher discharge capacity.

Conclusions

In conclusion, we have successfully constructed PMIA-PU membranes showing superior electrolyte wettability and excellent thermal dimensional stability for use in high power LIBs via electrospinning technique. Owing to the high porosity, electrolyte uptake and excellent electrolyte wettability, the PMIA-PU membranes are endowed with superior ionic conductivity of 1.38 mS cm^{-1}, high anodic stability up to 4.86 V. The incorporation of PMIA and the adjacent among fibers enable the membranes to exhibit robust tensile strength of 25.23 MPa, uniform pore size distribution and improved thermostability displaying 2% dimensional change after exposure to 180 ^{o}C for 0.5 h. Notably, the Li/LiFePO$_4$ (high mass loading LiFePO$_4$ electrode of 8 mg cm^{-2}) coin cells based on as-prepared PMIA-PU membranes except for the weight ratio of 2/8, exhibit higher cycling performance and better rate capability compared with Celgard membrane based cell, indicating that the PMIA-PU membranes might be potential separator candidates for high power LIBs. This work provides a versatile strategy for the further design and development of separators with robust mechanical strength and electrolyte wettability for LIBs.

Acknowledgements

Notes and references

^{a} State Key Laboratory for Modification of Chemical Fibers and Polymer Materials, College of Materials Science and Engineering, Donghua University, Shanghai 201620, China. E-mail: binding@dhu.edu.cn (B. Ding)
^{b} College of Biological, Chemical Sciences and Engineering, Jiaxing University, Jiaxing 314001, China
^{c} Key Laboratory of Textile Science & Technology, Ministry of Education, College of Textiles, Donghua University, Shanghai 201620, China
‡ These authors have contributed equally to this work.

1   M. Armand and J. M. Tarascon, *Nature*, 2008, **451**, 652.
2   C. Liu, F. Li, L. P. Ma and H. M. Cheng, *Adv. Mater.*, 2010, **22**, E28.
3   P. Arora and Z. Zhang, *Chem. Rev.*, 2004, **104**, 4419.
4   S. S. Zhang, *J. Power Sources*, 2007, **164**, 351.
5   H. Lee, M. Yanilmaz, O. Toprakci, K. Fu and X. Zhang, *Energy Environ. Sci.*, 2014, **7**, 3857.
6   P. Yang, P. Zhang, C. Shi, L. Chen, J. Dai and J. Zhao, *J. Membr. Sci.*, 2015, **474**, 148.
7   Y. Zhai, K. Xiao, J. Yu, J. Yang and B. Ding, *J. Mater. Chem. A*, 2015, DOI: 10.1039/c5ta00856e.
8   Y. Zhu, F. Wang, L. Liu, S. Xiao, Y. Yang and Y. Wu, *Sci. Rep.*, 2013, **3**, 3187.
9   S. H. Ju, Y. S. Lee, Y. K. Sun and D. W. Kim, *J. Mater. Chem. A*, 2013, **1**, 395.
10 F. Lian, Y. Wen, Y. Ren and H. Guan, *J. Membr. Sci.*, 2014, **469**, 67.
11 H. Y. Liu, L. L. Liu, C. L. Yang, Z. H. Li, Q. Z. Xiao, G. T. Lei and Y. H. Ding, *Electrochim. Acta*, 2014, **121**, 328.
12 J. Zhang, L. Yue, Q. Kong, Z. Liu, X. Zhou, C. Zhang, Q. Xu, B. Zhang, G. Ding, B. Qin, Y. Duan, Q. Wang, J. Yao, G. Cui and L. Chen, *Sci. Rep.*, 2014, **4**, 3935.
13 Q. Xu, Q. Kong, Z. Liu, X. Wang, R. Liu, J. Zhang, L. Yue, Y. Duan and G. Cui, *ACS Sustainable Chem. Eng.*, 2014, **2**, 194.
14 X. Wang, B. Ding and B. Li, *Mater. Today*, 2013, **16**, 229.
15 X. Wang, B. Ding, G. Sun, M. Wang and J. Yu, *Prog. Mater. Sci.*, 2013, **58**, 1173.
16 X. Huang, *J. Membr. Sci.*, 2014, **466**, 331.
17 Q. Wang, W. Song, L. Wang, Y. Song, Q. Shi and L. Fan, *Electrochim. Acta*, 2014, **132**, 538.
18 W. Chen, Y. Liu, Y. Ma and W. Yang, *J. Power Sources*, 2015, **273**, 1127.
19 J. Zhang, Z. Liu, Q. Kong, C. Zhang, S. Pang, L. Yue, X. Wang, J. Yao and G. Cui, *ACS Appl. Mater. Interfaces*, 2013, **5**, 128.
20 J. Lin, B. Ding, J. Yang, J. Yu and S. S. Al-Deyab, *Mater. Lett.*, 2012, **69**, 82.
21 L. Zhou, Q. Cao, B. Jing, X. Wang, X. Tang and N. Wu, *J. Power Sources*, 2014, **263**, 118.
22 S. W. Choi, J. R. Kim, Y. R. Ahn, S. M. Jo and E. J. Cairns, *Chem. Mater.*, 2007, **19**, 104.
23 Y. Zhai, N. Wang, X. Mao, Y. Si, J. Yu, S. S. Al-Deyab, M. El-Newehy and B. Ding, *J. Mater. Chem. A*, 2014, **2**, 14511.

ARTICLE

24 Y. Liang, S. Cheng, J. Zhao, C. Zhang, S. Sun, N. Zhou, Y. Qiu and X. Zhang, *J. Power Sources*, 2013, **240**, 204.

25 J. Hao, G. Lei, Z. Li, L. Wu, Q. Xiao and L. Wang, *J. Membr. Sci.*, 2013, **428**, 11.

26 J. Shi, Y. Xia, Z. Yuan, H. Hu, X. Li, H. Zhang and Z. Liu, *Sci. Rep.*, 2015, **5**, 8255.

27 J. Shi, T. Shen, H. Hu, Y. Xia and Z. Liu, *J. Power Sources*, 2014, **271**, 134.

28 F. Huang, Y. Xu, B. Feng, Y. Su, F. Jiang, Y. Hsieh and Q. Wei, *ACS Sustainable Chem. Eng.*, 2015, **3**, 932.

29 Y. Zhu, S. Xiao, Y. Shi, Y. Yang and Y. Wu, *J. Mater. Chem. A*, 2013, 1, 7790.

30 Y. Zhu, S. Xiao, Y. Shi, Y. Yang, Y. Hou and Y. Wu, *Adv. Energy Mater.*, 2014, **4**, 1300647.

31 J. J. Woo, S. H. Nam, S. J. Seo, S. H. Yun, W. B. Kim, T. Xu and S. H. Moon, *Electrochem. Commun.*, 2013, **35**, 68.

32 J. Zhang, L. Yue, Q. Kong, Z. Liu, X. Zhou, C. Zhang, S. Pang, X. Wang, J. Yao and G. Cui, *J. Electrochem. Soc.*, 2013, **160**, A769.

33 J. Chen, S. Wang, L. Ding, Y. Jiang and H. Wang, *J. Membr. Sci.*, 2014, **461**, 22.

34 X. Tang, Y. Si, J. Ge, B. Ding, L. Liu, G. Zheng, W. Luo and J. Yu, *Nanoscale*, 2013, **5**, 11657.

35 H. R. Jung and W. J. Lee, *Electrochim. Acta*, 2011, **58**, 674.

36 Y. Zhai, K. Xiao, J. Yu and B. Ding, *Electrochim. Acta*, 2015, **154**, 219.

37 T. Muraliganth and A. Manthiram, *J. Phys. Chem. C*, 2010, **114**, 15530.

38 R. Prasanth, V. Aravindan and M. Srinivasan, *J. Power Sources*, 2012, **202**, 299.

39 M. Raja, N. Angulakshmi, S. Thomas, T. P. Kumar and A. M. Stephan, *J. Membr. Sci.*, 2014, **471**, 103.

40 H. Song, N. Zhao, W. Qin, B. Duan, X. Ding, X. Wen, P. Qiu and X. Ba, *J. Mater. Chem. A*, 2015, **3**, 2128.

Nano-net structured PMIA-PU separators
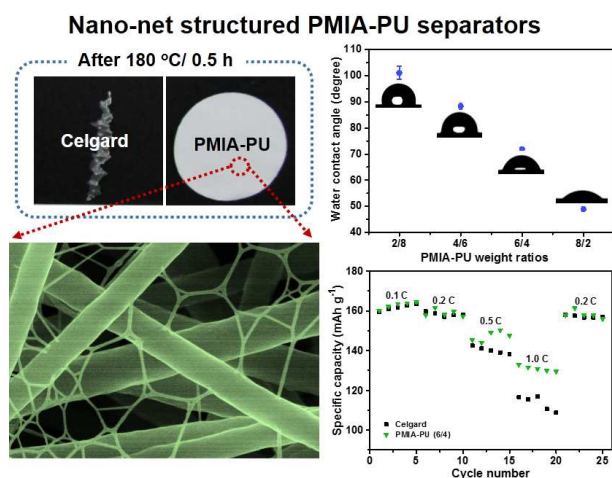
Nanonet-structured poly(*m*-phenylene isophthalamide)-polyurethane nanofibrous membranes for high power lithium ion batteries are fabricated via one-step electrospinning technique, which show enhanced thermostabilities and nonflammability as well as good wettability.